PCCP

Accepted Manuscript

ROYAL SOCIETY OF CHEMISTRY

www.rsc.org/pccp

From cellulose fibrils to single chains: understanding cellulose dissolution in ionic liquids

Xueming Yuan, Gang Cheng*

College of Life Science and Technology, Beijing University of Chemical Technology, North 3rd Ring East, #15, Chaoyang, Beijing, 100029, China

*Corresponding author: Email: gchengbuct@gmail.com; chenggang@mail.buct.edu.cn ; cell phone: 86 13693276690

Abstract: Cellulose is the most abundant and renewable organic compound on earth, it is however not soluble in common organic solvents and aqueous solutions. Cellulose dissolution is a key aspect to promote its value-added applications. Ionic liquids (ILs) have been shown to solubilize cellulose under relatively mild conditions. The easy processability of cellulose with ILs and their environmentally friendly nature prompted research in various fields such as biomass pretreatment and conversion, cellulose fiber and composite production, chemical conversion of cellulose in ILs. Progress has been made on understanding the mechanism of cellulose dissolution in ILs, including the structural characteristics of the ILs that are cellulose solvents, however many details remain unknown. In light of rapid development and importance of cellulose dissolution in the field of IL-based cellulose and biomass processing, it is necessary to provide an overview of current understanding of cellulose dissolution in ILs and outline possible future research trends. Recent literature studies suggest that synergistic effects between the anions and the cations of the ILs need to be revealed, which requires refining the structure of cellulose elementary fibrils, simulation of more realistic cellulose fibrils and detailed studies on the solution structure of cellulose in ILs. After analyzing literature studies, three interacting modules are identified, which are crucial to understand the process of cellulose dissolution in ILs: 1) structure of elementary fibrils; 2) solvation of cellulose in ILs; 3) solution structure of cellulose solubilized in ILs. A coherent analysis of these modules will aid in better design of more efficient ILs and processes.

1. Introduction

In light of foreseeable depletion of fossilized organic matter that have been providing human being with energy and chemical products, science and technology continue to move toward renewable resources and environmentally friendly processes.[1-3] Cellulose, hemicelluose and lignin are of growing importance in the development of alternative chemicals and fuels. Cellulose is mainly used in paper industry and a small fraction of it is used for regenerated fibers, films and synthesis of cellulose derivatives. [4] Cellulose does not melt upon heating and it is not soluble in common aqueous solutions or organic solvents, which make cellulose processing a challenging task.[5, 6] Until recently, cellulose was only dissolved in a few complex solvents via either derivatization or direct dissolution. Typical cellulose solvents include N-methylmorpholine N-oxide (NMMO), LiCl/N,N-dimethylacetamide (LiCl/DMAc), tetrabutylammonium fluorides/dimethyl sulfoxide mixture (TBAF/DMSO), etc. Among these solvents, only NMMO is used on an industrial scale to make cellulose fibers and the process is known as the Lyocell process.[5, 6] Before this environmentally friendly Lyocell process was commercialized in 1990s, the viscose process was widely used to manufacture cellulose fibers. [6] The viscose process consists of three main steps: 1) treating cellulose with sodium hydroxide; 2) derivatizing the treated cellulose with carbon disulfide resulting in a highly viscous sodium xanthogenate solution; 3) regenerating cellulose from the sodium xanthogenate solution with acids. [6]

Great progress has been made on understanding the mechanism of cellulose dissolution in these solvent systems.[7-16] Several reviews on cellulose dissolution in non-derivatizing solvents were published recently.[7-11] It is believed that the native hydrogen bonding network in cellulose needs to be disturbed or destroyed to enable cellulose dissolution.[8, 16] This is supported by the fact that partial substitution of the hydroxyl groups leads to cellulose derivatives that are often soluble in common solvents.[16, 17] As an example, the proposed mechanism of cellulose dissolution in LiCl/DMAc is briefly introduced here. ^{13}C NMR studies show that the lithium cations form coordination with the DMAc molecules and the chloride anions possess appropriate basicity to form hydrogen bonds with the cellulose hydroxyls. Association of the chloride anions produces a negatively charged cellulose chain and the cellulose chains are forced apart due to the charge repulsion.[18] Spange et al have measured the Kamlet-Taft solvatochromic parameters of DMAc/lithium halide binary systems.[19] The Kamlet-Taft parameters include the hydrogen bond basicity or acceptor ability (β), the hydrogen bond acidity or donor ability (α) and dipolarity-polarizability (π^*).[20] The hydrogen bond basicity of 5wt.% LiCl/ DMAc system has been determined to be 1.90, which is larger than that of 5wt.% LiBr/DMAc system that cannot dissolve cellulose.[19] In addition to hydrogen bonds, Medronho et al point out that the hydrophobic interaction between cellulose chains and solvents needs to be considered as well. [8, 9]

ILs consist of bulky organic cations and smaller inorganic or organic anions (Fig. 1). [6] ILs remain liquid at temperatures below 100ºC due to poorly coordinated anions and cations. ILs possess unique physicochemical properties such as low melting point, low vapor pressure, good thermal and chemical stability, which are desired for many processes.[6] In 2002, Swatloski et al reported a study of cellulose dissolution in ILs that later attracted lots of attention.[21] Certain ILs solubilize cellulose at relatively mild conditions. A typical example is 1-ethyl-3-methyl imidazolium acetate (EmimAc) that dissolves cellulose (Avicel PH101) up to 20wt.% at room temperature within one hour.[22] The easy processability of cellulose with ionic liquid and its environmentally friendly nature prompted research in various fields such as biomass pretreatment and conversion, IL-based biomass fractionation, cellulose fiber and composites production, chemical conversion of cellulose in ILs. [6, 23-25]

In 2006, two groups reported that the enzymatic hydrolysis rates of cellulose were improved after treating cellulose (Avicel PH 101)[26] and steam-exploded wheat straw[27] with 1-butyl-3-methyl imidazolium chloride (BmimCl). During a biochemical conversion of lignocellulosic biomass into fuel molecules, a pretreatment step is currently necessary to improve the enzymatic hydrolysis efficiency

due to inherent biomass recalcitrance.[25, 28] In plant cell walls, semi-crystalline cellulose fibers are embedded in a lignin-hemicelluose matrix. The purpose of biomass pretreatment is to improve cellulose accessibility to enzymes and remove lignin.[29] Different pretreatment techniques have been developed, including physical, chemical, physiochemical, biological approaches, etc.[28] Biomass pretreatment accounts for about 20% of total cost of the biochemical conversion process.[30] Therefore, an efficient pretreatment technique with lower cost is desirable. After about 10 years' development, the IL pretreatment process (Fig. 2) has become one of the leading pretreatment techniques and the number of scientific reports exploring various aspects of the IL pretreatment process have been increasing steadily [31]. During a typical IL pretreatment process, the biomass and IL are mixed according to predetermined mass ratio and kept at an elevated temperature for a certain amount of time. After that, the biomass slurry is diluted with water to precipitate dissolved cellulose and to wash out the IL from the biomass. The pretreated biomass is then subjected to enzymatic hydrolysis either in wet or dry state.

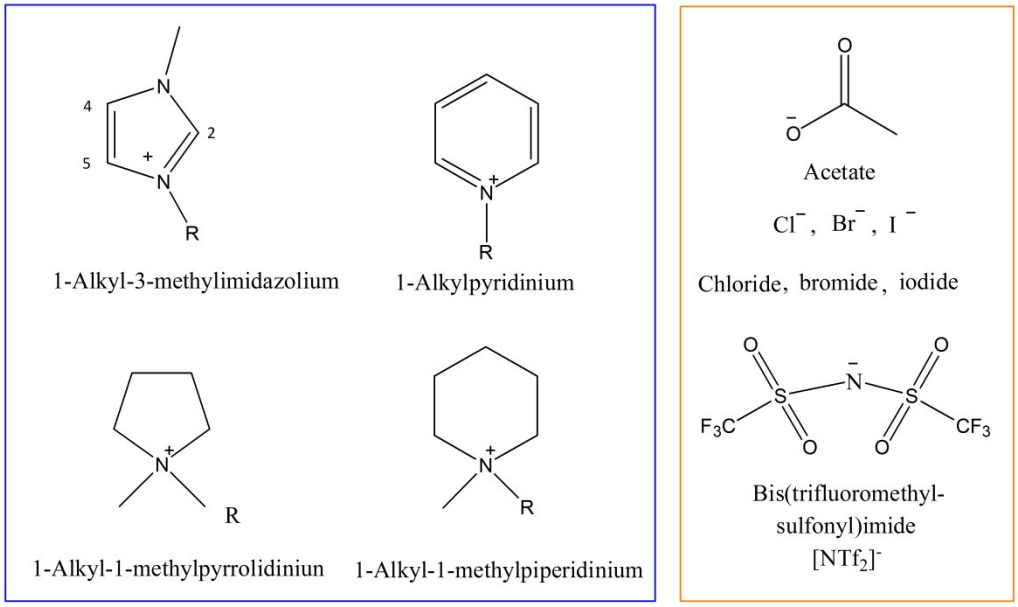

Fig.1 Chemical structures of the cations and anions of representative ILs.

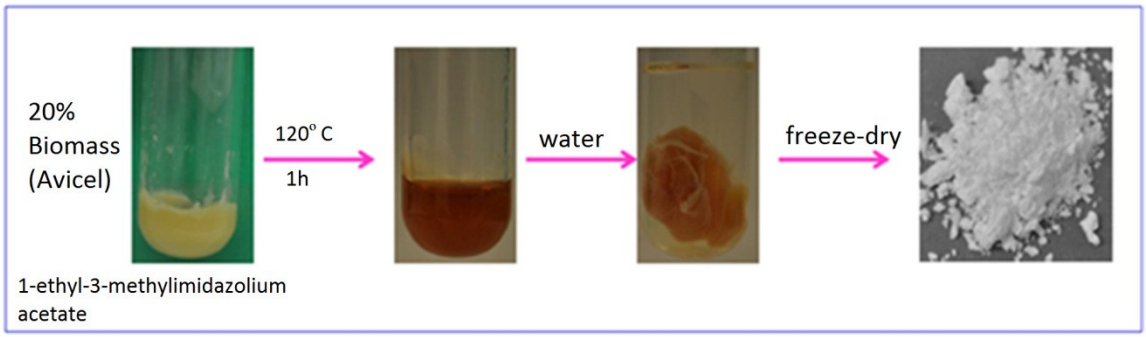

Fig.2 A typical IL pretreatment process.

Although the IL pretreatment holds promise for biomass conversion on industrial scales, many problems remain to be solved. Among them are high production cost, high viscosity, low biocompatibility and recyclability.[25, 31] This requires development of efficient pretreatment solvents that are cheap, biocompatible, of lower viscosity and easy to recycle. Attempts have been made to synthesize biocompatible ILs to pretreat biomass, such as choline-based ILs, amino acid-based ILs and poly(ethylene glycol)-functionalized ILs. [32-36]

It is essential to understand the mechanism of cellulose dissolution in ILs in order to develop more efficient ILs for biomass pretreatment and processing. Investigations on the mechanism of cellulose dissolution in ILs started soon after Swatloski's report.[37, 38] Computer simulations, NMR studies and solubility tests have greatly improved our knowledge on this topic. As a result of that, several review articles have been published. [5, 6, 23, 25, 39, 40, 31, 41] In this review, we would like to focus on the process of cellulose dissolution in ILs instead of the structural characteristics of the ILs that lead to cellulose solvation. The latter has been analyzed recently. [6, 31, 41]

It is generally accepted that the anions of the ILs form hydrogen bonds with the hydroxyl groups of cellulose destroying native hydrogen-bonded network in cellulose crystals.[31, 41] A quantitative measure of the IL's hydrogen bond acceptor capacity, mainly controlled by the anion, is by the β parameter evaluated via the Tamlet-Taft equations.[42,20] A computer simulation study shows that the value of the β parameter increases when the cation-anion interaction strength is weakened.[43] The solubility of cellulose in ILs correlates with the β parameter where a higher value leads to solubilization.[18, 31] For example, the BmimAc has a β value of 1.201 and it is cellulose solvent while the $BmimNTf_2$ has a value of 0.248 and it is not cellulose solvent.[44] Addition of water to the ILs decreases the β value and the solubility of cellulose in them.[42, 45] Another simulation work shows that the anion's hydrogen bond acceptor capacity is affected by its charge density and steric hindrance effect [46]; this explains the correlation between the structure of the anions and the corresponding ILs' cellulose solvation power.

In comparison to the anion, the role of the cation in dissolving cellulose is more controversial. [6, 31, 41] Interactions between the cations of imidazolium-based ILs and cellulose have been proposed as "hydrogen bond" [47], "van del walls interaction" [48], "hydrophobic interaction" [49] or "no specific interaction" [37]. A quantitative measure of the contribution of the anion to cellulose dissolution is given by the α parameter, derived from the Tamlet-Taft equations. The α parameter is mainly determined by the cation of the IL, although the anion-cation interaction is believed to influence it as well. In one study, the value of the β parameter was kept roughly constant, the cellulose solubility increased with increase of the value of the α parameter.[47] This was attributed to the hydrogen bonds formed between the imidazolium cations and cellulose. In another work, a combined parameter, (β-α), was proposed to incorporate the contribution of the cations to cellulose dissolution.[44] Based on cellulose solubility data in different ILs, an empirical "dissolution window" was found with the values of (β-α) between 0.35 and 0.90.[44] The literature data of the α and β parameters for different ILs that were used for cellulose and biomass processing have been compiled in a recent review paper.[31] Interested readers should consult that paper for more details.

Literature studies have shown that synergistic effects between the anion and the cation needs to be revealed[50] in order to fully understand cellulose dissolution in ILs. This requires a multi-scale investigation of the interaction between ILs and cellulose.[41] The multi-scale investigation is determined by the supra molecular structure of cellulose, as will be described in section 2.1. Another important aspect is the conformation of cellulose chains in IL solutions. This has been mostly derived from rheological studies that were not included in previous review papers. By analogy to the dissolution of semi-crystalline polymers in organic solvents, a conjectured process of cellulose dissolution in ILs is proposed here. The cellulose dissolution is a process which begins with IL molecules contacting the surfaces of cellulose fibers. This is followed by diffusion of IL molecules into cellulose fibers that cause swelling and subsequent disintegration of cellulose chains as a concerted action between the cations and the anions. Finally, molecularly dispersed cellulose chains or aggregates of cellulose chains constitute the cellulose/IL solutions. The proposed process of cellulose dissolution needs further analysis of the literature studies and more experimental work. In light of rapid development and importance of cellulose dissolution in the field of IL-based cellulose and biomass processing [6, 23, 25, 31, 40, 51-53], it is

necessary to provide an overview of previous studies that are relevant to understand the interactions between cellulose and ILs and outline possible future research directions.

This review begins with presenting current knowledge of the structure of cellulose fibrils that forms the basis of understanding cellulose dissolution (section 2). The structure of elementary fibrils have been mostly studied by NMR, x-ray diffraction (XRD), small angle x-ray and neutron scattering (SAXS and SANS). This is followed by analyzing the literature work of the cellulose/IL interactions that occur from the molecular level to fibrillar level (section 3). The cellulose/IL interactions have been investigated by computer simulation, NMR and XRD. The conformation and aggregation of cellulose chains in ILs, studied mainly by rheology, will be introduced in section 4. A discussion that integrates the structure of cellulose elementary fibrils, interactions between IL and cellulose and the solution structure will be presented in section 5.

2. Hierarchical structure of cellulose in plant cell walls

2.1 Cellulose elementary fibril, microfibril and macrofibril

Cellulose is a linear homopolymer composed of repeat units of cellobiose. The degree of polymerization (DP) of cellulose is given by the number of anhydro glucose units (AGUs). The cellulose chain has a reducing end with a hemiacetal hydroxyl group on the pyranose ring and a non-reducing end. The presence of hydroxyl groups and oxygen atoms on the pyranose rings promote parallel packing of cellulose chains to crystallize into elementary fibrils. Native cellulose crystal structure is called cellulose I, which has two polymorphs, a triclinic structure I_α and a monoclinic structure I_β.[54] Cellulose I_α is enriched in most alga and bacteria and I_β is dominant polymorph in higher plants.[55] In cellulose I_α, there is one chain in a triclinic unit cell while there are two conformationally distinct chains in a monoclinic unit cell of cellulose I_β.

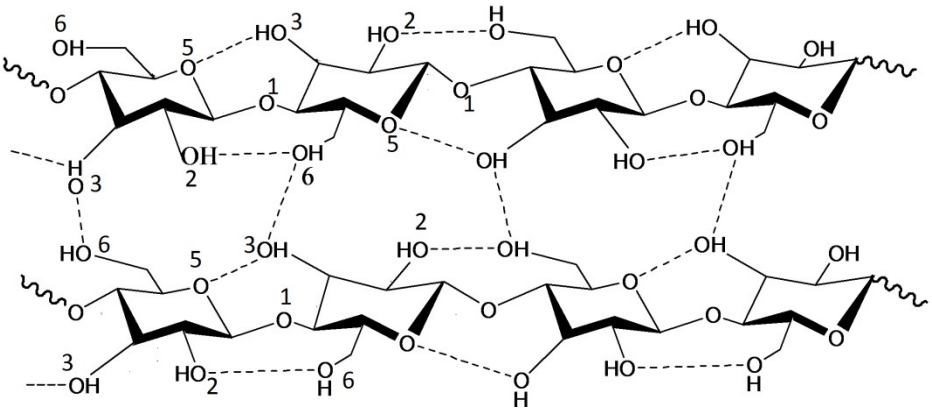

Fig. 3 Inter and intra molecular hydrogen bonds in cellulose I_β . (Adapted from Ref. 47).

In each AGU, there are three hydroxyl groups and one oxygen atom on the ether group that can serve as hydrogen bond donor or acceptor (Fig. 3). There are two types of intra-molecular hydrogen bonds in cellulose I_β: O3−H·····O5, O2−H·····O6 and one inter-molecular hydrogen bond: O6−H·····O3.[54] The hydrophobic interactions and C−H·····O bonds hold the hydrogen-boned sheet together in cellulose crystals. Powder XRD pattern of cellulose I_β is usually characterized by three major peaks.[22] The main peak at around 22.5° of (200) plane is indicative of the distance between hydrogen-bonded sheets in cellulose I. There is a broad peak at ~16°, which is known to be a composite of two peaks (16.7° and 14.9°) from I_β that correspond to $(1\bar{1}0)$ and (110) planes respectively. The third small peak at 34.5° of (004) plane corresponds to 1/4 of the length of one cellobiose unit and arises from ordering

along the fiber direction. It is sensitive to the alignment of the chains into fibrils. Both the crystallite size and the moisture content in the samples can affect the observed diffraction peaks .[22]

In plant cell walls, cellulose exists as different levels of structures, i.e., single cellulose chains, elementary fibrils (consisting of tens of single cellulose chains), macrofibrils (bundles of elementary fibrils) and cellulose fibers (Fig. 4).[56] Ding et al propose that the macrofibril is formed by a number of newly synthesized elementary fibrils.[57, 58] As the cell grows, the macrofibrils may split to form individual microfibrils consisting of a single elementary fibril associated with non-cellulosic polymers like hemicelluloses. In other words, elementary fibrils and macrofibrils contain only cellulose while the microfibrils contain both cellulose and non-cellulosic polymers. It is noted that others consider a microfibril as consisting of a number of elementary fibrils.[55] In this context, we refer a microfibril as an elementary fibril associated with non-cellulosic polymers.

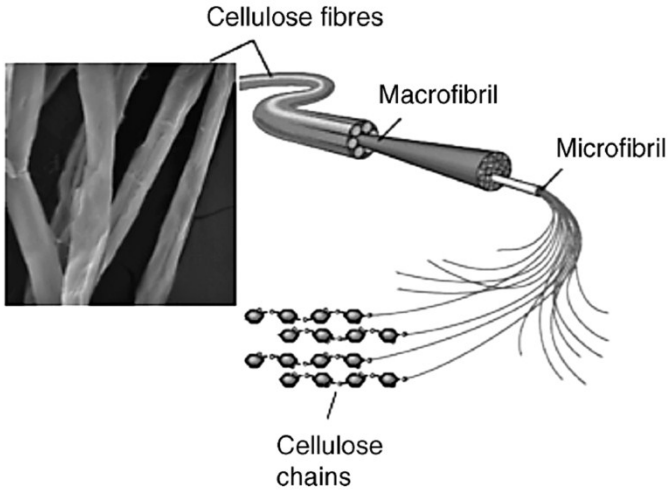

Fig. 4 Hierarchical morphology of a plant cellulose fiber. (Reproduced from Ref. 56).

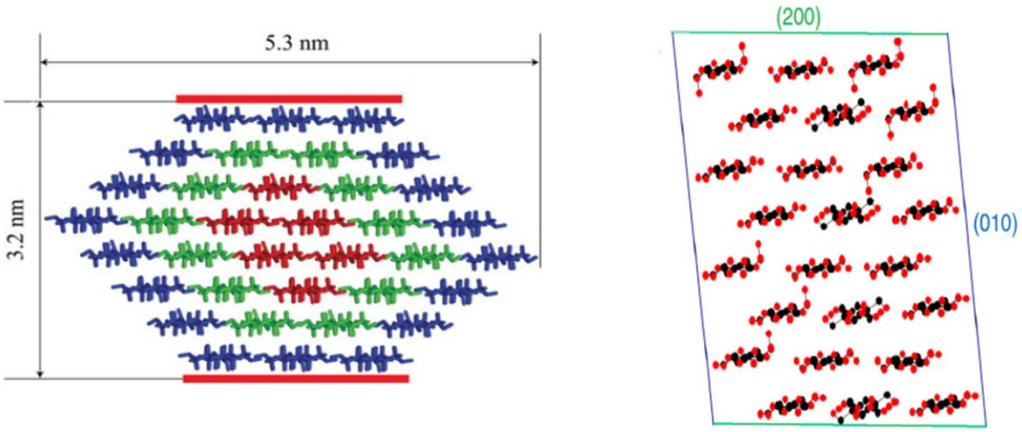

Fig. 5 Schematic models of 36-chain and 24-chain cellulose elementary fibrils based on cellulose I structure. (Reproduced from Ref. 58 and 71)

A popular model structure of cellulose synthase complex in higher plants consists of six-membered rosettes with each member composed of six cellulose synthase proteins.[57, 59] It is suggested that each cellulose synthase protein synthesizes one β-glucan chain and a rosette produces 36 chains that form one elementary fibril. High resolution AMF analysis of fibrillar structures in cell walls of corn stover stem shows that the widths of elementary fibrils are slightly larger than those predicted from a 36-chain model.[60] The measured widths are 3.3±0.5nm in vertical direction and 5.7±0.9 nm in horizontal

direction. Calculated dimensions of a transverse section based on the cellulose I_β structure are 3.2 and 5.3 nm. The deviation in sizes was attributed to the AFM tip broadening and elementary fibrils association with matrix polymers.[60]

The diameters of the elementary fibrils or microfibrils have been measured by NMR, wide angle x-ray scattering (also called XRD), SAXS, and more recently studied by wide angle neutron scattering (WANS) and SANS.

2.2 NMR Measurement

From solid state NMR spectra, the lateral dimensions of the elementary fibrils are evaluated by comparing the contributions from cellulose chains buried within the fibrils and chains exposed at the surface of the fibrils in the C-4 region.[61, 62] In the ^{13}C spectrum, the signals from crystalline cellulose are centered on 89 ppm, and around 84 ppm are a group of signals which can be assigned to cellulose chains in different environment from that of crystalline chains.[62, 63] The signals from crystalline cellulose are considered as superposition of two doublets stemmed from the I_α and I_β forms [62], and this assignment is depending on the relative abundance of I_α and I_β. Some researchers suggest a further signal overlapping these and assign it to "paracrystalline" cellulose.[62, 64] Paracrystalline cellulose is considered as less ordered than I_α and I_β allomorphs, but more ordered than amorphous chains.[65] In a ^{13}C NMR analysis of bleached softwood kraft pulp, the proportion of paracrystalline cellulose was reported to be 37%, estimated by non-linear spectral fitting with a combination of Lorentzian and Gaussian functions.[65]

The broader upfield signals centered on 84 ppm have been assigned to chains at fibril surface and/or to amorphous regions within the elementary fibrils.[62, 66] The ^{13}C NMR spectroscopy of cellulose in onion and quince showed a double peak centered on 84ppm that was assigned to surface chains in an ordered conformation.[62] A broad underlying band centered at 85ppm was assigned to disordered cellulose chains. Both the surface chains and disordered cellulose chains were found to be located outside the crystalline chains whose NMR signals were centered at 89 ppm.[62] Cellulose chains presented on surfaces are often less constrained with respect with conformations they can adopt.

Using NMR spectroscopy and molecular modeling, Viëtor et al showed that in higher plants cellulose surface chains had a different C-6 conformation so that O-6 was not in the correct position for the hydrogen bond from O-2.[63]. In the amorphous region, cellulose chains are free to adopt a wider range of conformations than those in the crystalline lattice.

Newman exploited the differences in proton rotating-frame relaxation time constants T1ρ between cellulose and amorphous lignin-hemicellulose matrix and generated proton spin-relaxation edited NMR spectrum.[61] A sub-spectrum of crystalline cellulose was obtained and used for the estimation of the fraction of cellulose chains contained in the interiors of crystallites. A parameter X was defined as [61] :

$$X = (\text{area between 87 and 93 ppm})/(\text{area between 80 and 93ppm}) \qquad \text{Eq. (1)}$$

Further analysis concluded that the signal near 85 ppm was from surface chains alone. By assuming a square cross-section for the elementary microfibrils, the lateral dimension is related to X by [61] :

$$L = 2h/(1 - X^{1/2}) \qquad \text{Eq. (2)}$$

where h is the thickness of the layer of surface chains. The parameter X represents the fraction of interior chains of the elementary fibrils. An approximation of h = 0.57nm was taken as the average of the spacings between (110) planes and $(1\bar{1}0)$ planes.[61]

In cases where reliable spectrum deconvolution is difficult or proton spin-relaxation edited NMR spectrum processing is unsuccessful [67, 68], the signals from crystalline chains and surface chains are separated using cutoff chemical shifts. For example, in a study of cotton microcrystalline cellulose the area between 93.9 and 86.2ppm was chosen to represent the contribution from crystalline chains, and the area between 86.2 and 80.3ppm was attributed to that of the surface chains.[68] The area ratio between interior chains and surface chains was related to the geometry and dimensions of the elementary fibrils. As shown in Fig. 6, a square cross-sectional shape was assumed and the lateral dimension was calculated by Eq. 2. In Fig. 6, the elementary fibril consisted of 36 chains with (110) and $(1\bar{1}0)$ terminating surfaces. Thickness of the surface layer was estimated by taking the average of d-spacings of (110) and $(1\bar{1}0)$ planes. In another study of celery collenchymas cellulose, the chemical shift that separated interior chains and surface chains was chosen as 86.5ppm, with a further cutoff at 82.7ppm to remove the hemicellulose shoulder. [67]

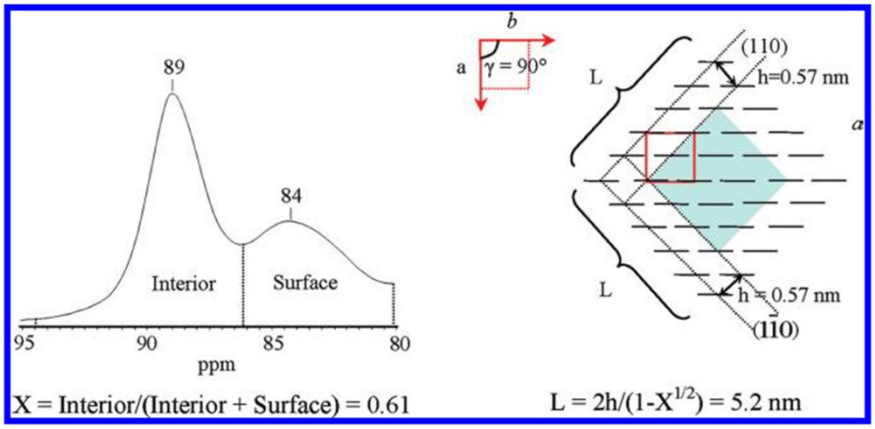

Fig.6 Evaluation of the dimensions of elementary fibrils by ^{13}C NMR spectroscopy. (Reproduced from Ref. 68)

To summarize, in order to calculate the lateral dimensions of an elementary fibril from the NMR data, the following structural features need to be known or assumed: 1) less ordered cellulose chains are positioned at surfaces of the fibrils; 2) proper separation of C-4 signals into contributions from interior chains and surface chains; 3) cross-sectional shape of an elementary fibril; 4) the thickness of the surface layer is known or can be calculated based on crystallographic data of crystalline cellulose.

The C-4 signals have also been used to estimate the crystallinity of cellulose, i.e., the fraction of crystalline cellulose which equals to the parameter *X*. [69] In this case, the broader upfield signal is assigned to the C4 of disordered cellulose as well as to the surface chains. The interior of the crystallites is considered to be "crystalline" and the term "amorphous" is used to describe the remaining less ordered chains including surface chains .[69]

Although there are NMR evidences [62, 70, 71] to support the organization of cellulose chains corresponding to the upfield C-4 signal as a fringe on the fibril surfaces, other experimental studies show a structure of alternating crystalline and amorphous domains along the elementary microfibril in higher plants.[55] In NMR studies of cellulose elementary fibrils, the surface chains have been described as "ordered" [62], "less ordered" [71] or "amorphous" [69]. A WANS study of elementary fibrils in the primary cell walls from collenchymas suggests that surface chains are packed laterally in the same way and at almost the same mean spacings as in the crystalline regions, despite the differences in hydrogen bonding and

conformation.[71] NMR has been proven useful to study the structure of elementary fibrils; however, complementary information is sometimes needed before reaching meaningful conclusions.[61, 67, 71]

2.3 WAXS measurement

WAXS is another popular technique used for the estimation of lateral dimensions of elementary fibrils.[61, 67, 71-74] The WAXS method is based on the Scherrer's equation which relates the full width at half maximum (FWHM) of a diffraction peak to the number of crystallographic plane corresponding to that diffraction peak or the thickness of the crystallographic planes.[75] The peak width decreases with increasing in the number of the crystallographic plane and a limited number of planes result in broadening of the diffraction peak. The Scherrer's equation is given by [75] :

$$B_{hkl} = K\,\lambda/(\beta\cos\theta) \quad \text{Eq. (3)}$$

where B_{hkl} is the thickness of the crystallite perpendicular to the (hkl) plane, K is the Scherrer's constant, λ is the wavelength of the x-ray radiation, β is FWHM and θ is the diffraction angle. The Scherrer's constant depends on the shape of the crystallites, the size distribution of the crystallites and the lattice plane.[76] Since the variation of the constant is modest, values between 0.90 and 1.0 are often used.[75, 77] Application of the Scherrer's equation is complicated by the instrument broadening and the lattice disorder-induced broadening of the diffraction peaks. The instrumental broadening can be measured experimentally using standard samples such as powdered lanthanum hexaboride. The corrected FWHM is given by [72] :

$$\beta_{corr} = \sqrt{\beta_{exp}^2 - \beta_{std}^2} \quad \text{Eq. (4)}$$

Where the β_{corr}, β_{exp} and β_{std} represent the corrected, sample's and the standard sample's FWHM, respectively. A further correction for the effect of lattice disorder is not trivial. It can be done by introducing defects into model elementary fibrils and comparing the calculated diffractogram with the one measured experimentally.[75] However, if the (400) reflection can be measured, the disorder-related broadening is estimated by assuming that the width of the reflections increases with the square of the reflection order.[71] The intercept of the plot of FWHM vs. the square of the reflection order for the 200 and 400 peaks is taken as the FWHM that is corrected for disorder.[71] In cases where the instrument broadening and/or the disorder-related broadening are not corrected, the lateral sizes obtained from the Scherrer's equation are considered as a lower bound.

2.4 SAXS and SANS measurements

Small angle scattering, including SAXS and SANS, measures structural units which are larger than typical lattice spacing (~1Å). The application of SAXS and SANS to cellulose elementary fibrils has been summarized in a recent review [29], thus only essential features of SAS will be introduced here. SAS data contains structural information of the scattering objects and the interactions between them. A typical SAS setup can only measure the cross-section of elementary fibrils because the length of them (~1μm) is usually outside the measurement range of SAS. Analysis of the SAS data relies on modeling of the scattering curves with proper scattering functions, which depend on the shape, size and interaction of the scattering objects. When the interaction between objects is small, for example, when cellulose elementary fibrils are separated far away from each other, this term can be dropped out of the scattering functions. A typical example of such analysis is demonstrated in a study of elementary fibrils from various wood species, cotton and flax.[72] In that study, elementary fibrils were modeled as infinite long cylinders with different cross-sectional shapes. For spruce wood samples, a two-dimensional paracrystal model was used as an interference function while for other samples an interference function

seemed unnecessary, judged by the appearances of the scattering curves. The SAXS data analysis suggested that the shape of the elementary fibrils could be of circular, rectangular and elliptical, depending on the biomass origins. In another work, the elementary fibrils from celery collenchyma were analyzed by SAXS. [67] A distinct interference peak was observed on the SAXS curve, which was modeled using a modified Lennard-Jones potential utilizing only the repulsive force. The fit to the experimental data did not produce a unique set of parameters, which is not uncommon in SAS analysis. In that work, the high background was believed to make the analysis unreliable.[67] In addition to the background, the scattering from other structural features in the biomass samples such as voids can also complicate the data analysis.[72]

The presence of a distinct peak on the scattering curves indicates a higher packing density of the elementary fibrils in cell walls. Unless the packing is regular enough to constitute a crystalline superlattice, only one Bragg peak is observed.[71] The average center-to-center spacing of the elementary fibrils can be extracted from the peak position q* via $2\pi/q^*$. The center-to-center distance is an upper limit for the elementary diameter.[67] It approximates the mean diameter only when the elementary fibrils are in close contact with each other.[71] On the other hand, if the elementary fibrils are in close contact with each other, there will be little room for non-cellulosic materials like hemicelluloses, and therefore the scattering contrast for SAXS measurement may not be large enough to generate useful data. There are a few studies where SANS was used to measure the center-to-center distance of elementary fibrils on spruce wood [67] and celery collenchyma [78]. In those studies, the center-to-center distance was believed to represent the mean diameter of the elementary fibrils. That is to say, the elementary fibrils were closely packed and the contrast between elementary fibrils and the matrix was high enough to permit sensible measurements. It is noted that in SANS experiment the contrast was enhanced by hydrating spruce wood samples using D_2O or H_2O, however for celery collenchyma samples the contrast was good enough to extract the center-to-center distance without using D_2O or H_2O.[78]

2.5 Summary

NMR is sensitive to chain conformation while WAXS and WANS are more sensitive to long range chain packing. The lateral sizes derived from the NMR measurements include the surface layer and it is generally assumed that the chains on the surface also contribute to the Scherrer dimensions. In the study of cellulose elementary fibrils from Collenchyma, WANS data showed that the surface chains were packed laterally in the same way and at almost the same mean spacings as in the crystalline regions, despite the differences in conformation as shown by NMR. SANS and SAXS measure the shape, size and packing of elementary fibrils provided the contrast between fibrils and the surrounding matrix polymers is enough. In the presence of a distinct scattering peak on the SANS or SAXS curves, a center-to-center distance can be extracted from the peak position and it servers as upper limit value of the diameter of the elementary fibrils. It approximates the diameter if the fibrils are closely packed.

The structural features of elementary fibrils and its mechanism of synthesis remain subjects of continuing research and debate.[59] As shown in Table 1, based on the size of the elementary fibrils estimated by different techniques, models containing 36 [60], 24 [71] and 18 [75] chains have been proposed for cellulose elementary fibrils from different biomass species. The spatial distribution of amorphous domains within an elementary fibril is also not resolved, with models of crystalline core surrounded by amorphous shell at its surface and of alternating crystalline and the amorphous domains along the fibril present in literature (Fig. 7).

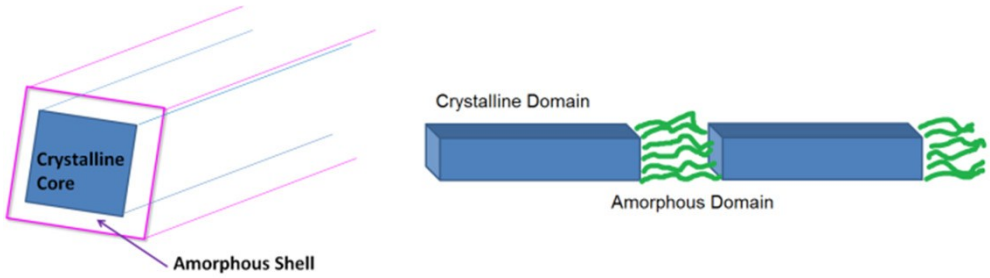

Fig. 7 Possible structures of elementary fibrils

Table 1. Representative studies of the elementary fibril measured by different techniques

Biomass type	SAXS/SANS(nm)	WAXS(nm)	NMR(nm)	AFM(nm)	Elementary Fibril Model
Spruce wood [73]	2.5±0.2	(200), (1-10) and (110) 2.2±0.2			
Norway spruce compression wood[74]	3.0±0.8	(200), 2.9			
Norway spruce wood[72]	2.6	(200), 3.0			36-chain
Cotton microcrystalline cellulose[68]		(200), 4.8	5.2		
Sitka spruce[71]	3.0, center-to-center distance	(200),3.29±0.13;(1-10) and (110), 2.6±0.1			24-chain, rectangular cross section
Celery collenchyma[67]	3.6, center-to-center distance	(200), 2.4	2.6		15- to 25-chain
Celery collenchyma[78]	2.9-3.0, center-to-center distance	(200),3.2;(1-10) and (110), 2..5			24-chain, rectangular cross section
Eucalyptus wood[61]		(200), 3.5	3.8		
Corn stover stem[60]				5.3 x 3.2	36-chain, diamond-shaped cross section
Mung bean[75]		(200), 2.5	average number of chains per (200) sheet derived		18-chain

3. Cellulose dissolution in ILs without and with co-solvents

3.1 Interactions between cellulose and ILs

Pioneering studies of cellulose dissolution focused on solvation of glucose and cellubiose in ILs. The formation of hydrogen bonds between hydroxyl protons on sugar and the anion on ILs has been confirmed by computer simulations [38] and NMR studies [37]. In a molecular dynamics study of glucose

solvation in 1, 3-dimethylimidazolium chloride (DmimCl), Youngs et al., concluded that the most likely coordination number for glucose was four chloride anions, where three OH groups formed hydrogen bonds to three chloride anions and the remaining two bound to a fourth chloride which forms an OH----Cl----HO bridge.[38] Later, Youngs et al found a small presence of the cation in the primary solvation shell of the glucose with the association occurring through the weakly acidic hydrogen at the 2-position of the imidazolium ring interacting with the oxygen atoms of the sugar hydroxyls.[79] Interestingly, they also discovered that glucose molecules did not change the interactions and overall liquid structure of DmimCl. More recently, Youngs et al used neutron diffraction, NMR and molecular dynamics simulations to study dissolution of glucose in another IL, EmimAc.[80] Their primary objective was to examine the reason that cellulose was dissolved more rapidly in acetate-based ILs than the corresponding chloride-based ILs. They suggested that after initial separation of cellulose chains or strands through disrupting of the existing hydrogen-bonding, the cellulose chains might be reconnected via a chloride hydrogen bond bridge. So this second hydrogen bonding system needed to be destroyed before cellulose chains could be separated again. This was not the case for acetate anions since the hydrophobic methyl group reduced the chances of the secondary hydrogen bonding system. NMR data suggested that there was no direct interaction between sugar hydroxyl groups and acidic hydrogen on the imidazolium ring.[80]

Although it is generally accepted that the anion of the ILs plays a dominate role in cellulose dissolution, the contribution of the cation is still not resolved, i.e., the nature of the interaction between the cation and cellulose.[6] Remsing et al. used ^{13}C and $^{35/37}Cl$ NMR relaxation measurement to reveal the dissolution mechanism of cellobiose and glucose in BmimCl.[37] The NMR relaxation data suggested there was no specific interaction between the IL cation and the sugar. Youngs et al. reported the presence of weak interactions between glucose hydroxyl groups and acidic hydrogen on the imidazolium ring in the DmimCl [79] while no such interaction was found in the EmimAc [80].

Liu et al studied solvation of cellulose oligomers in EmimAc using molecular dynamics simulation. The cations were found to be in close contact with the cellulose oligomers through hydrophobic interactions.[49] The stacking of imidazolium cations with glucose rings was not observed.[49] Gross et al., calculated the density distribution of the chloride anions and Bmim cations around the dissolved cellulose chains with a DP of 16.[81] It was discovered that the chloride anions formed strong hydrogen bonds with the hydroxyl groups of cellulose in both the equatorial and axial directions, thus replacing both the intra- and inter-molecular hydrogen bonds that existed in cellulose crystals prior to dissolution. The imidazolium ring of the Bmim cations had closer contacts with ether oxygen atoms and CH groups along the axial direction than with groups along the equatorial direction. The results suggested that both the anion and cation of BmimCl interacted with cellulose chains along the axial direction which further implied disruption of the inter-sheet (hydrogen-bonded sheets) contacts in cellulose crystals.[81] The spatial distribution of the cations and anions around dissolved cellulose chains were also investigated in another simulation work. Rabideau et al. proposed that cations interacted with anions that were hydrogen-bonded to cellulose surface through electrostatic interactions, while interacting with nonpolar domains of cellulose via dispersion forces (Fig. 8).[48] The formation of cation-anion chains and networks at cellulose surface allowed minimum disturbance of the IL bulk connectivity. [48]

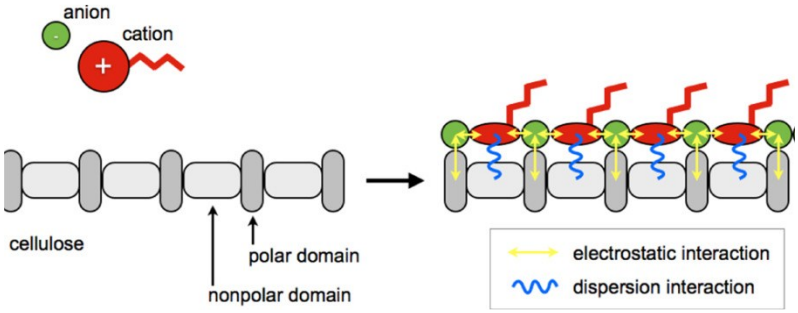

Fig. 8 Distribution of the cation and anion along a dissolved cellulose chain. (Reproduced from Ref. 48)

A better understanding of cellulose dissolution in ILs requires studies that focus on synergistic interactions between anion and cation of ILs and on dissolution of large cellulose fibrils. In one work, cellulose I_β crystal was constructed with 384 unit cells in a simulation box.[82] Gupta et al found that solvation led to the breaking of hydrogen bonds at the cellulose surface.[82] Mostofian et al. performed all-atom molecular dynamics simulations of a cellulose elementary fibril in BmimCl.[50] A 36-chain model was used to construct the elementary fibrils with a DP of 20. The role of the cation in the solvation of cellulose was clearer in this study. The results suggested that Bmim cations interacted with cellulose in two different ways, stacking on cellulose strands on the hydrophobic surfaces, for example, the (200) plane and intercalation in between cellulose strands on hydrophilic surfaces, for example, the $(1\bar{1}0)$ plane. It was believed that both interactions facilitated cellulose dissolution by loosening layers of the cellulose structure.[50]

The breakup of small bundles of cellulose I_α and I_β was studied in BmimCl, EmimAc, and 1,3-dimethylimidazolium dimethylphosphate (DmimDMP).[83] Anions bound to the hydroxyl group of cellulose, forming negatively charged moieties. Cations then associated with these attached anions wedging themselves between cellulose strands, leading to strand separation. Although this study was done for cellulose bundles with 6 and 8 cellulose chains, a 36-chain bundle was also found to follow the same pattern of breakup.[83] This process is similar to one of the suggestions about the mechanism by which cellulose dissolves in a mixture of LiCl/DMAc.[8]

The interactions between cellulose and ILs were also studied by XRD. Analysis of the variations of the major peaks on XRD data as a function of pretreatment condition produces information which aids in understanding the process of cellulose solubilization in ILs. Cheng et al. studied the process of solvation of pure cellulose and cellulose in lignocellulosic biomass using EmimAc and BmimAc.[22, 84, 85] With increasing treatment severity, the most dramatic change in the XRD spectrum was the reduction in intensity of the broad secondary peak centered on 16° until it vanished (Fig. 9a and 9b). The diminishing of the secondary peak indicates the following: 1) decreasing in cellulose crystallinity or increase of disorder; 2) disturbance of the organization of cellulose chains within the hydrogen-bonded sheets in cellulose I_β ; 3) preferential interaction of IL molecules with the $(1\bar{1}0)$ and (110) planes. Molecular dynamics simulations of a cellulose elementary fibril in BmimCl showed that the hydrophilic $(1\bar{1}0)$ plane was a preferred site of interaction with IL.[86] The simulation also suggested intercalation of the cations in between cellulose strands on hydrophilic surfaces.[50] A slight shift to lower angle of the main peak was observed in prior studies (see Fig. 9) and it was explained as a result of the intercalation of the IL molecules into the gap between hydrogen bonded sheets.[22] It is noted that the shift of the main peak to lower angles was also expected for transforming into cellulose II or amorphous structures. [22]

A recent study on the effect of cationic structure of ILs with varied cationic backbones and alkyl chains on the dissolution of microcrystlline cellulose found that the acidic protons on the heterocyclic rings may form hydrogen bonds with cellulose, and this was essential for the dissolution.[47] The solubility data further suggested that the cation of the ILs could decrease cellulose solubility if the interaction between cation and anion was strong. It was suggested that the steric hindrance effect of alkyl chains in the cations of the ILs might also decrease the cellulose solubility. [47]

Thermodynamically the process of cellulose dissolution means the free energy change of this process is negative. Gross et al. calculated the free energy change of dissolution of a 36-chain elementary fibril in BmimCl.[87] In BmimCl, separating cellulose chains to the dissociated state led to an entropy reduction

of the solvent. This indicated that some solvent molecules were bound to cellulose chains. As a result of that, the intra-molecular degree of freedom of cellulose chains was also reduced upon dissociation. However, the overall entropy change was positive. The internal energy change of cellulose dissolution was negative at the temperatures studied. Therefore the free energy change was favorable for cellulose dissolution in BmimCl. [87] This is consistent with an experimental study of the heat of dissolution of cellulose in EmimAc. Andanson et al. used a precision semi-adiabatic solution calorimeter to measure the enthalpy of dissolution of microcrystalline cellulose and reported a value of -132±8 Jg^{-1}.[88] The interactions between fifteen ILs and cellobiose were also measured by a high-precision solution microcalorimetry.[89] A good correlation was found between the heat of mixing measured and the solubility behavior of cellulose.

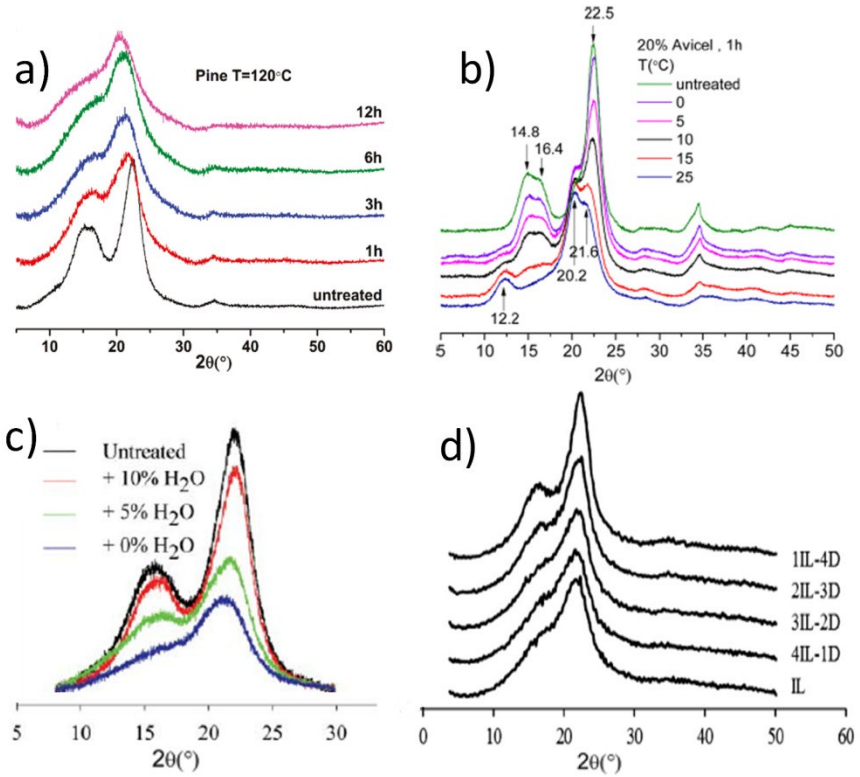

Fig. 9 XRD data of pine samples treated with EmimAc (a); Avicel samples treated with EmimAc(b); maple wood samples treated with BmimAc/water mixture solvents (c) and eucalyptus wood samples treated with EmimAc/DMSO mixture solvents(d). (Reproduced from Ref. 84, 22, 42 and 90, respectively)

3.2 Interactions between cellulose and ILs with co-solvents

Although some ILs are solvents for cellulose, the high cost and viscosity limit their applications. One of the approaches to tackle this challenge is to add co-solvents to lower the cost and viscosity. Doherty et al used EmimAc, BmimAc, $BmimMeSO_4$ and water mixture solvents to treat maple wood flour.[42] The XRD data of the treated samples demonstrated that addition of water to the IL had the similar effect on cellulose crystalline structure as that of lowering pretreatment temperature and decreasing treatment time. The dramatic change in the secondary peak and the slow variation in the main peak with reduction of water content were demonstrated (Fig. 9c). This was also the case for EmimAc/DMSO mixture solvents with increasing the EmimAc concentration (Fig. 9d).[90]

Addition of certain amount of DMSO and other organic solvents to EmimAc produced similar or enhanced biomass pretreatment performances compared with using pure EmimAc, which was attributed to lower viscosity of the mixture solvent system.[90, 91] Further insights into the effects of DMSO on the cellulose/IL interactions have been offered by computer simulations. In one work, a crystal was constructed with 8×8 cellulose chains with a DP of 8 for each chain. Huo et al showed that there was enhancement of the interaction between chloride ions and cellulose in the presence of DMSO, despite the number of chloride ions decreases due to dilution.[92] Using molecular dynamics simulations and quantum chemistry calculations, Zhao et al suggested that the DMSO promoted the dissociation of EmimAc by solvation of the cation and anion.[93] The dissociated anion became more easily interacting with cellulose to improve the dissolution of cellulose. In that work, a cellulose chain with DP of 10 was used.[93] On the other hand, a combined study of viscosity, ionic conductivity and MD simulations concluded that DMSO did not induce cation-anion dissociation in BmimAc.[94] Furthermore, simulation studies showed that DMSO did not interact specifically with glucose in a mixture solvent of 1:1 molar ratio.[94] In a more recent study, a cellulose elementary fibril was constructed with a 36 chains organizing into 8 sheets, and each chain had a DP of 10.[95] Velioglu et al pointed out that DMSO had the role of an "innocent" co-solvent which did not interfere with the interactions between cellulose and BmimAc.[95] It simply lowered viscosity and led to faster mass transport and dissolution. The calorimetric study of cellulose dissolution in EmimAc/DMSO mixture solvent also indicated that DMSO did not affect significantly the interactions between cellulose and EmimAc.[88]

3.3 Summary

Studies on cellulose dissolution in ILs can be divided into two aspects, 1) correlating the structures of anions and cations of the ILs with cellulose solubility; 2) exploring the process of cellulose dissolution in cellulose solvents such as BmimCl and EmimAc. It has come to a consensus that both the cation and anion contribute to the corresponding IL's solvation power for cellulose. Similar to other cellulose solvents, the replacement of the native hydrogen bonds in cellulose crystals with that formed between the IL and individual cellulose chains is essential for dissolution. The hydrogen bond donor capacity of the anion and the hydrogen bond acceptor ability of the cation have been assessed by the Kamlet-Taft equation. In addition to hydrogen bond, the interactions between the cation and the cellulose chains have also been described as "hydrophobic" and "van del walls interactions".

From glucose to elementary fibrils, computer simulation work contributes significantly to our understanding of the interactions between cellulose and ILs on different length scales. However, coordinated actions between anions, cations and cellulose chains that lead to dissolution remain to be revealed. XRD data show that IL interacts strongly with the $(1\bar{1}0)$ and (110) planes. In comparison, the stacking of the (200) plane seems to be more recalcitrant to ILs. A scheme that involves association of anions onto cellulose chains via hydrogen bonds seems to share similarities with the proposed process of dissolution of cellulose in LiCl/DMAc. The charged cellulose chains are forced apart and go into solutions. Addition of DMSO to the IL solution reduces its viscosity that leads to a faster dissolution of cellulose. This is beneficial to cellulose processing and biomass pretreatment.

ILs are versatile chemicals on which the structures of the cation and anion can be independently modified, enabling tenability of their properties. The viscosity of some of the ILs can be reduced by introducing certain functional groups, such as alkoxy groups.[96] A reduction in viscosity is advantageous for cellulose dissolution.[97, 98] Incorporation of alkoxy chains onto the ethyl group of EmimAc leads to reduced viscosity while still exhibiting remarkable solubility for cellulose.[97] However, if the size of the functionalized cations becomes large enough, a drastic reduce in cellulose solubility is observed.[97] Possible reasons are as follows: 1) A larger cation effectively reduces the anion molar concentration;[36] 2) the presence of the basic oxygen atoms in the side chain of the cation may interfere with hydrogen

bonding of the anion with cellulose;[6] 3) the change in overall IL's hydrophobicity.[36] When a hydroxyl group is appended to the end of the side chains, ILs dissolves much less cellulose than their analogues.[97] This could be due to the competition with cellulose in forming hydrogen bonds with the anion. In addition, ILs comprised of dialkoxy-functionalized ammonium cations[99] and poly(ethylene glycol)-functionalized ammonium cations[36] have also been reported to be able to dissolve cellulose.

It is worthy to mention that depolymerization[100] and decomposition[101, 102] of cellulose incubated in EmimAc and EmimCl at high temperatures have been reported. Clough et al. found that the C-2 carbon of the imidazolium ring reacted with the aldehyde functionality on the open chain sugar to cause modifications of both cellulose and the EmimAc.[102] This poses challenges for recycling of the ILs and analyzing the pretreated biomass samples.

4. Solution structure of cellulose in ILs

4.1 Rheological studies

Understanding of the mechanism of cellulose dissolution in ILs also requires information on the structure of cellulose in IL solutions, i.e. whether cellulose chains are molecularly dispersed or aggregating. Up to now, the solution structure of cellulose in ILs has mainly been investigated by rheology. Rheological studies of cellulose solutions in ILs reveal molecular conformation and organization of cellulose, which is crucial to understand the mechanism of cellulose dissolution and also important in many industrial processing operations involving a rapid change of shapes such as fiber spinning. The characterization and analysis of can be divided into four categories based on the literature studies. [103-112]

1. Newtonian fluid and shear thinning behavior. Most of the polymer solutions exhibit shear thinning property at large shear rates, meaning that the viscosity decreases as shear rate is raised. Shear thinning behavior occurs since polymer chains in a solution can disentangle, stretch and orient themselves parallel to the driving force, or the shear can break up the aggregated structures that exist in polymer solutions.[113] In most cases, with increase of cellulose concentration, shear thinning behavior (Fig. 10) was observed and the Newtonian plateau limit shifted to a lower frequency, similar to reports for most solutions of neutral polymers. [104, 106] In some studies only a Newtonian behavior was observed over a wide range of shear rates. This might be because of lower DP of cellulose used and experimental difficulties encountered at high shear rates.[105, 110] Other studies reported only the shear thinning behavior that was attributed to the aggregated structures (gels and liquid crystalline structures) formed in concentrated cellulose solutions.[107, 112]

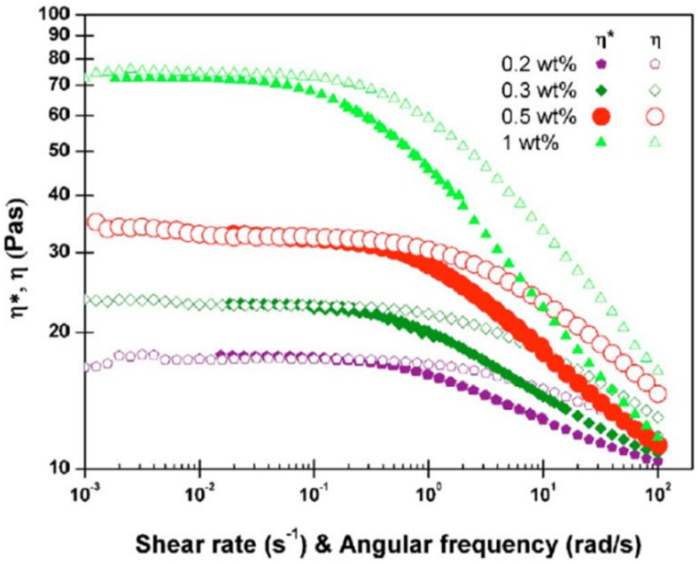

Fig. 10 Shear rate dependence of steady shear viscosity and frequency dependence of complex viscosity of cellulose/BmimCl solutions. (Reproduced from Ref. 108).

2. The empirical Cox-Merz rule states that for linear viscoelastic materials the magnitude of the complex viscosity is the same as the steady shear viscosity at equal values of frequency and shear rate. [104, 108] Different results from the Cox-Merz plots have been reported for cellulose/IL solutions. In a study of cellulose pulp dissolved in EmimAc [111], the Cox-Merz rule held well for the cellulose solutions with concentrations of 0.2 to 8 wt.% in a frequency range of 0.1 to 100s^{-1}. Usually the deviations from the Cox-Merz rule are due to breakup of the aggregates in solutions by steady shear, and this will lead to a lower steady shear viscosity since the small strain applied during oscillatory experiment is less effective in breaking down the aggregates.[114] In many cases, the Cox-Merz rule applied to cellulose solutions only in the Newtonian regime, while in the shear thinning regime the steady shear viscosity was larger than the complex viscosity.[104, 108, 109] Such an example is shown in Fig. 10. Therefore the unusual result that shear viscosity is larger than the complex viscosity is hard to understand. It suggests a structural transition occurs in cellulose solutions of which the nature is still not clear. Chen et al pointed out that this indicated that cellulose/BmimCl solutions were perhaps not simply neutral polymers in the θ regime.[108] It is noted that the usual deviation from the Cox-Merz rule was also reported for cellulose/BmimCl solutions with concentrations of 6 to 14 wt.% .[106]

3. Storage modulus and elastic modulus vs. frequency. The storage and loss modulus are usually determined as a function of the frequency at constant amplitude in the linear viscoelastic range. Fig. 11 shows a typical example of frequency dependence of loss (G') and storage (G'') modulus of cellulose/BmimCl solutions. At lower cellulose concentrations, G' is always smaller than G'' and no crossover is found within the test frequency range. This suggests that the majority of the energy is dissipated by viscous flow and the solution exhibits a liquid-like behavior. With increase of cellulose concentration, the $G'$and G'' are becoming close in the higher frequency range and the slope over which reflects the dynamics of the cellulose chains. Detailed analysis of dynamics of polymer chains in solutions and in melts is rather complex and it will not be introduced here due to limit of space. Interested readers may consult text books for details.[115] With further increase of cellulose concentration, a crossover occurs in the higher frequency region and it moves to lower values as the cellulose concentration increases. This indicates that gel-like or solid-like behavior due to entanglement of cellulose chains in solutions with higher concentration. At low frequencies the scaling $G' \sim \omega^2$ and $G'' \sim$

ω is expected for unentangled polymer solutions.[116] High polydispersity and/or a weakly aggregated structure in the solutions cause deviation from this scaling. [108]

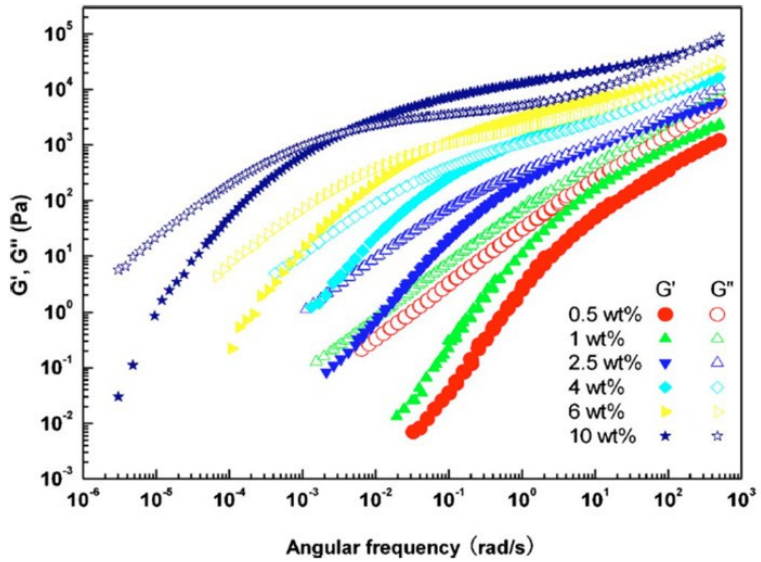

Fig. 11 Frequency dependence of loss and storage modulus of cellulose/BmimCl solutions. (Reproduced from Ref. 108).

4. Dilute, semi-dilute unentangled and semi-dilute entangled solutions. The definitions of dilute and semi-dilute polymer solutions, unentangled and entangled solutions can be found in textbooks of polymer physics.[115] A plot of zero-shear viscosity or specific viscosity vs. cellulose concentration allows one to determine the overlap concentration and the entanglement concentration (see Fig. 12 for an example). The scaling exponents in the semi-dilute regime (c*) and in the entangled semi-dilute regime (c_e) reflect the solvent quality of the IL for the cellulose that dissolves in it. If the solvent mediated attraction between monomers just balances the effect of steric repulsion (hard-core repulsion), the polymer chain will adopt a random walk conformation and a solvent under such a condition is called the θ-solvent. If the attraction between monomers is weaker than the hard core repulsion, the polymer chain swells and this corresponds to a good solvent. The exponents should be 1, 2 and 14/3 respectively for polymers in θ-solvents, and 1, 1.3 and 3.9 for polymers in good solvents.[115] Based on this approach, literature studies concluded that AmimCl, BmimCl and EmimAc were θ-solvents for cellulose (Table 2).

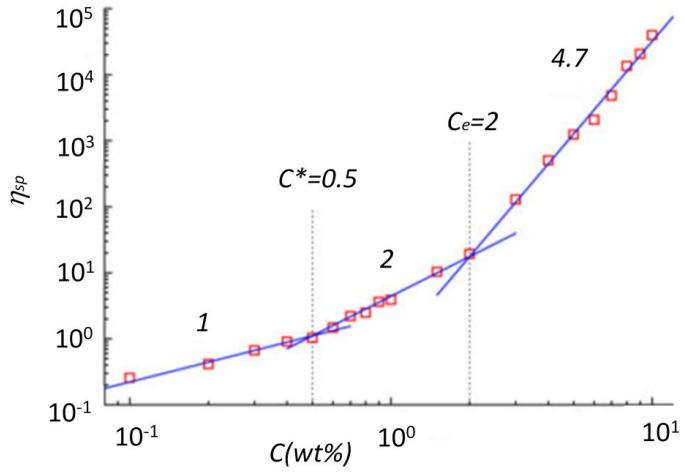

Fig. 12 Concentration dependence of specific viscosity of cellulose/EmimAc solutions. (Reproduced from Ref. 109).

Table 2 Rheological studies of cellulose/IL solutions

IL	Source of Cellulose	Measurement Temperature(°C)	Solution Concentration	Shear Rate or Angular Frequency (s^{-1})	Flow Behavior	Solvent Quality
AmimCl[112]	wood pulp cellulose(DP=530)	100	10 to 25 wt.%	0.1 to 1000	Shear thinning observed; Newtonian not observed	
AmimCl[104]	dissolving pulp(DP=220)	30	0.1 to 3.0 wt.%	0.01-100	Newtonian and shear thinning observed	θ
BmimCl[103]	dissolving pulp (DP=670)	90	3 to 15 wt.%	0.1-100	Shear thinning character increased from 2 to 15 wt.%	
BmimCl[106]	cellulose pulp(DP=505, 1100)	90	6 to 14 wt.%	~0.05 to ~400	Newtonian and shear thinning observed	
BmimCl[108]	α-cellulose (DP=741)	25	0.1 to 10 wt.%	~ 10^{-5} to ~ 1000	Newtonian and shear thinning observed	θ
BmimCl, EmimAc[105]	microcrystalline cellulose(DP=300) spruce sulfite pulp (DP=1000) bacteria cellulose (DP=4420)	20 and 100 for spruce sufite pulp in EmimAC; 40 for microcrysalline cellulose in BmimCl and EmimAC	0.1 to 15wt.%	0.001 to 1000	Newtonian behavior observed over 2-3 decades of shear rates; solution ejected at high shear rates	θ
BmimCl, EmimAc[117]	Avicel Ph101 (DP=180)	EmimAc Solution, 0 to 100C;BmimCl solution, 70 to 130	~0.1 to 15wt.%	0.1 to ~400	Newtonian behavior observed	
EmimAc[107]	microcrystalline cellulose(DP=220)	25	5 to 18 wt.%	0.01 to 100	Newtonian behavior for 5 and 7 wt.% solutions; slight shear thinning observed for 10 and 12 wt.% solutions; Newtonian plateau disappeared for higher concentrated solutions due to gelatin	
EmimAc[111]	cellulose pulp(DP=860)	25	0.1 to 8 wt.%	0.1 to 100	Newtonian and shear thinning observed	θ
EmimAc[109]	α-cellulose (DP=850)	25	0.1 to 10 wt.%	0.01 to 100	Newtonian and shear thinning observed	θ

The solvent quality for linear neutral polymers can also be derived from the scaling relation between the radius of gyration, R_g, and the molar mass, $R_g \sim M_w{}^{\nu}$. In θ-solvents, $\nu = 0.5$ and the polymer chain has a random walk conformation. In good solvents, $\nu = 0.588$ and the polymer chain is swollen. The R_g of polymer chains is calculated using intrinsic viscosity via the Fox-Flory equation:

$$R_g^2 = \left(\frac{1}{6}\right)\left[\left(\frac{[\eta]}{\Phi}\right)M\right]^{2/3} \quad \text{Eq. (5)}$$

Where M is polymer molecular weight, $\Phi = 2.8 \times 10^{23}$mol is the Flory constant. The molecular weight dependence of the R_g of cellulose in different IL solutions were collected[105, 109, 111] and plotted in Fig 13. It shows that the value of R_g varies with DP of cellulose as $R_g \sim \mathrm{DP}^{0.42}$, and the exponent is less than

0.5. Note that due to limited number of data points used to extract the exponent, the error is expected to be larger than those extracted from viscosity-concentration plots.

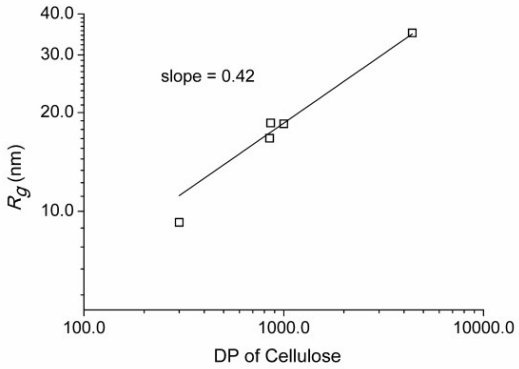

Fig. 13 Molecular weight dependence of the R_g of cellulose in different IL solutions. (Data adapted from Ref. 105, 109 and 111).

The solvent quality of mixture solvents of AmimiCl, BmimCl, EmimCl and DMSO were also investigated by rheological studies. The results showed that addition of DMSO could decrease the viscosity of the ILs but it did not change the solvent quality for cellulose. The mixture solvents of AmimCl/DMSO, BmimCl/DMSO and EmimCl/DMSO are θ-solvents for cellulose at 25ºC. [118, 119]

4.2 Scattering studies

In principle the conformation of cellulose chains in IL solutions can be studied by scattering techniques, such as static and dynamic light scattering, SAXS and SANS. Light scattering has been used to study the structure of cellulose and its derivatives dissolved in other solvents such as DMAc/LiCl, NMMO, cadmium oxide in aqueous trans(2-aminoethyl)amine(Cd-tren).[15] The ratio between radius of gyration and hydrodynamic radius serves as a measure of the architecture of the objects.[16] In general it decreases with increasing compactness due to contraction, branching or aggregation. Aggregates of cellulose chains are often observed in cellulose solutions, and a fringed micelle model has been proposed that reflects the semi-crystalline structure of the native cellulose fibers.[15] Inability of the solvents to molecularly disperse cellulose chains leads to these structures. However, molecular dispersion can be achieved for cellulose in DMAc/LiCl [120] and in Cd-tren [14] with proper manipulation of the experimental conditions.

Light scattering study of cellulose/IL solution has been rarely reported.[121, 122] Possible reasons are as follows:1) the presence of the heterogeneities or nanostructures in some ILs that could interfere with light scattering measurement [117, 123]; 2) ILs are usually hygroscopic and the presence of water leads to formation of aggregates [124, 125] that interfere with light scattering measurement. In a light scattering study of cotton cellulose (DP=2400) in AmimCl, the R_g was determined to be 75nm via the Zimm plot and AmimCl was considered as a good solvent for cellulose.[121] This is not consistent with the rheological studies. The larger size of cellulose chains was caused by the negative charges they carried as measured by the zeta potential. It was proposed that chloride ions associated with cellulose chain by hydrogen bonding and each cellulose chain can be considered as a polyelectrolyte. This is direct evidence that shows accumulation of anions around cellulose chains. More zeta potential measurements are thus expected.

Recently, SANS, SAXS and static light scattering were used to study cellulose dissolved in EmimAc/DMF (dimethyl formamide) solutions.[126] The results suggest that EmimAc/DMF is a good solvent for cellulose. Deuterated DMF was used in SANS experiment to enhance the contrast between

the solvent and cellulose. Measurement of cellulose in ILs by SANS cannot produce useful data without using either deuterated ILs or deuterated cellulose, both of which are not easily accessible.

4.3 Summary

Most rheological studies of cellulose/IL solutions show that some of the ILs are θ-solvents for cellulose. Thermodynamically ILs are not better cellulose solvents than traditional ones such as cupric hydroxide in aqueous ethylenediamine (cuen), LiCl/DMAc. Neutral linear polymers assume a random walk conformation in θ-solvents. Some studies suggest that cellulose chains are semi-flexible. A polymer chain can be treated as consisting of N Kuhn segments that are freely jointed. Assuming a random walk conformation, the average end-to-end distance is given by $\sqrt{Nb^2}$, where b is the length of a Kuhn segment. A Kuhn length of 4.8nm was obtained for cellulose (DP=860) dissolved in EmimAc at 25°C, that is larger than some common polymers such as polyethylene (b=1.4nm), polypropylene (b=1.1nm).[111] However, in another study of α-cellulose (DP=850) solubilized in EmimAc, the Kuhn length was determined to be 0.25nm, indicating rather flexible cellulose chains.[109] With increasing cellulose concentration, cellulose chains associate and form gel and liquid crystalline phases that exhibit shear thinning behaviors.

Cellulose/IL solutions exhibit unusual behaviors that need to be studied further. The deviation from the Cox-Merz rule suggests that cellulose chains are not like other common neutral linear polymers in the θ regime. The light scattering study of cotton cellulose (DP=2400) in AmimCl demonstrates that AmimCl is a good solvent, contrary to rheological studies. Based on an SANS investigation, the EmimAc/DMF is concluded as a good solvent, which is also inconsistent with rheological studies on IL/DMSO solutions.

5. Summary and Outlook

Improved knowledge of cellulose dissolution in ILs aids in better design of next generation ILs that hold promise in cellulose processing, chemical modification of cellulose, biomass pretreatment, etc. Cellulose dissolution is a multi-step process which involves adsorption and diffusion of IL molecules into cellulose fibrils, swelling of cellulose fibrils by ILs and separation of cellulose chains. Progress has been made on understanding the mechanism of cellulose dissolution in ILs, however many aspects remain unknown. Understanding the mechanism of cellulose dissolution in ILs requires further refining the structure of elementary fibrils, investigating coordinated action of the cations, anions and cellulose chains, and exploring the solution structures of cellulose in ILs.

The structural features of elementary fibrils remain subjects of continuing research, that include the number of cellulose chains constituting one elementary fibril, its cross-sectional shape, the arrangement of amorphous cellulose chains. The differences in instrument sensitivity, biomass origins and inherent defects accompanied with thin cellulose fibrils contribute to the controversial data presented in literature.

The supra molecular structures of cellulose chains in plant cell walls dictate that the interactions between cellulose and IL molecules occur on different length and time scales. Computer simulations reveal many details of the interactions among the cations, anions and cellulose chains on the molecular level. Solubility data allow one to correlate the structures of the cations, anions with cellulose solvation power of the corresponding ILs. Association of anions to cellulose chains via hydrogen bonds has been suggested and the charge repulsion between different chains may have been involved in the process of separating cellulose chains. On the elementary fibril level, computer simulations show that cations stack on cellulose strands on the hydrophobic surface and intercalate in between cellulose strands on hydrophilic surfaces. This is consistent with the XRD data that suggest that the ordering of cellulose

chains within the hydrogen-bonded sheets is destroyed first and IL molecules insert into hydrogen-bonded sheets during the dissolution process. The 36-chain model is often adopted in computer simulation studies. The DP of the cellulose chains used in computer simulations is however usually less than 20, much smaller than that of the real cellulose chains. In order to obtain a clearer picture of the dissolution process, studies of larger systems are desired.

The solution structure of cellulose solubilized in ILs is not fully resolved yet. Rheological data of cellulose/IL solutions indicate that ILs are θ-solvents for cellulose, however they are not like normal neutral polymers in the θ-regime. The dissolved cellulose chains may behave like polyelectrolyte in ILs. More experimental studies are needed to measure the net charge on dissolved cellulose chains and their conformation. Imidazolium-based ILs are reported to have nano-structures as a result of segregation between the charged parts of cations and anions and the neutral parts of alkyl chains. Upon cellulose solvation, the entropy of ILs has been shown to be reduced; the interaction between cellulose chains and the nano-structures of ILs however has not been reported.

Addition of co-solvents such as DMSO does not change the solvent quality while it decreases its viscosity. A recent SANS study of cellulose in IL/DMF solutions however shows that the mixture solvent is a good solvent for cellulose. Future work involving rheological and scattering measurements are expected. It is worth to mention that SANS has been used in recent studies of the solution structures of methylcellulose in water.[127-129]

While computer simulations and analytical tools such as NMR, x-ray and neutron scattering, etc., have contributed greatly to our understanding of cellulose dissolution in ILs, applications of new methodology and complementary techniques are also important. With the aid of a solvent suppression technique, proton NMR signals of cellulose hydroxyl groups were observed in a non-deuterated IL, DmimDMP.[130] It was found that a strong interaction between the hydroxyl group at the 6-position of the AUG and the IL was a key step for cellulose dissolution.[130] Solution microcalorimetry was used to measure the affinity of cellobiose and ILs.[89] The heat of mixing was found to be a good indicator of cellulose solubility in ILs.[89] Cruz et al. used *in situ* viscosity measurement to study the rate of cellulose dissolution in a number of ionic liquids.[131] The IL 1-butyl-3-methylimidazolium ethanoate was found to dissolve cellulose faster than analogous ILs and the rate of dissolution was affected by both anion basicity and its relative concentration. [131]

Abbreviations: IL, ionic liquid; AGU: anhydro glucose unit;WAXS, wide angle x-ray scattering; SAXS: small angle x-ray scattering; SANS: small angle neutron scattering; EmimAc: 1-ethyl-3-methyl imidazolium acetate; BmimAc: 1-butyl-3-methyl imidazoliumacetate; BmimCl :1-butyl-3-methyl imidazolium chloride ; $BmimNTf_2$:1-buthyl-3-methylimidazolium bis((trifluoromethyl)sulfonyl)imide; DmimCl:1, 3-dimethylimidazolium chloride ;DmimDMP:1,3-dimethylimidazolium dimethylphosphate;DMAc: N,N-dimethylacetamide; NMMO: N-methylmorpholine N-oxide ;TBAF:tetrabutylammonium fluorides; DMF: dimethyl formamide; DP: degree of polymerization; Cd-tren: cadmium oxide in aqueous trans(2-aminoethyl)amine; cuen: cupric hydroxide in aqueous ethylenediamine

Acknowledgements

Gang Cheng acknowledges support for this research by the joint funds of National Natural Science Foundation of China and Large Scale Scientific Facility of Chinese Academy of Science (U1432109).

References:

1. A. J. Ragauskas, G. T. Beckham, M. J. Biddy, R. Chandra, F. Chen, M. F. Davis, B. H. Davison, R. A. Dixon, P. Gilna, M. Keller, P. Langan, A. K. Naskar, J. N. Saddler, T. J. Tschaplinski, G. A. Tuskan and C. E. Wyman, *Science*, 2014, **344**, 1246843.
2. R. A. Sheldon, *Green Chem.*, 2014, **16**, 950-963.
3. D. Esposito and M. Antonietti, *Chem. Soc. Rev.*, 2015, DOI: 10.1039/C4CS00368C.
4. D. Klemm, B. Heublein, H. P. Fink and A. Bohn, *Angew. Chem., Int. Ed.*, 2005, **44**, 3358-3393.
5. A. Pinkert, K. N. Marsh, S. Pang and M. P. Staiger, *Chem. Rev. (Washington, DC, U. S.)*, 2009, **109**, 6712-6728.
6. H. Wang, G. Gurau and R. D. Rogers, *Chem. Soc. Rev.*, 2012, **41**, 1519-1537.
7. B. Lindman, G. Karlström and L. Stigsson, *J. Mol. Liq.*, 2010, **156**, 76-81.
8. B. Medronho and B. Lindman, *Adv. Colloid Interface Sci.*, DOI: http://dx.doi.org/10.1016/j.cis.2014.05.004.
9. B. Medronho and B. Lindman, *Curr. Opin. Colloid Interface Sci.*, 2014, **19**, 32-40.
10. S. Sen, J. D. Martin and D. S. Argyropoulos, *ACS Sustainable Chem. Eng.*, 2013, **1**, 858-870.
11. A. Pinkert, K. N. Marsh and S. Pang, *Ind. Eng. Chem. Res.*, 2010, **49**, 11121-11130.
12. C. Zhang, R. Liu, J. Xiang, H. Kang, Z. Liu and Y. Huang, *J. Phys. Chem. B*, 2014, **118**, 9507-9514.
13. W. Burchard, *Biomacromolecules*, 2001, **2**, 342-353.
14. K. Saalwächter, W. Burchard, P. Klüfers, G. Kettenbach, P. Mayer, D. Klemm and S. Dugarmaa, *Macromolecules*, 2000, **33**, 4094-4107.
15. L. Schulz, B. Seger and W. Burchard, *Macromol. Chem. Phys.*, 2000, **201**, 2008-2022.
16. W. Burchard, *Cellulose*, 2003, **10**, 213-225.
17. E. Kontturi, T. Tammelin and M. Osterberg, *Chem. Soc. Rev.*, 2006, **35**, 1287-1304.
18. A. El-Kafrawy, *J. Appl. Polym. Sci.*, 1982, **27**, 2435-2443.
19. S. Spange, A. Reuter, E. Vilsmeier, T. Heinze, D. Keutel and W. Linert, *J. Polym. Sci., Part A: Polym. Chem.*, 1998, **36**, 1945-1955.
20. A. F. M. Claudio, L. Swift, J. P. Hallett, T. Welton, J. A. P. Coutinho and M. G. Freire, *Phys. Chem. Chem. Phys.*, 2014, **16**, 6593-6601.
21. R. P. Swatloski, S. K. Spear, J. D. Holbrey and R. D. Rogers, *J. Am. Chem. Soc.*, 2002, **124**, 4974-4975.
22. G. Cheng, P. Varanasi, R. Arora, V. Stavila, B. A. Simmons, M. S. Kent and S. Singh, *J. Phys. Chem. B*, 2012, **116**, 10049-10054.
23. S. J. Zhang, J. Sun, X. C. Zhang, J. Y. Xin, Q. Q. Miao and J. J. Wang, *Chem. Soc. Rev.*, 2014, **43**, 7838-7869.
24. M. Dashtban, A. Gilbert and P. Fatehi, *RSC Adv.*, 2014, **4**, 2037-2050.
25. A. Brandt, J. Grasvik, J. P. Hallett and T. Welton, *Green Chem.*, 2013, **15**, 550-583.
26. A. P. Dadi, S. Varanasi and C. A. Schall, *Biotechnol. Bioeng.*, 2006, **95**, 904-910.
27. L. Liu and H. Chen, *Chin. Sci. Bull.*, 2006, **51**, 2432-2436.
28. Y. Zheng, J. Zhao, F. Xu and Y. Li, *Progr. Energy Combust. Sci.*, 2014, **42**, 35-53.
29. G. Cheng, X. Zhang, B. Simmons and S. Singh, *Energy & Environmental Science*, 2015, **8**, 436-455.
30. B. Yang and C. E. Wyman, *Biofuels Bioproducts & Biorefining-Biofpr*, 2008, **2**, 26-40.
31. K. C. Badgujar and B. M. Bhanage, *Bioresour. Technol.*, 2015, **178**, 2-18.
32. K. Ohira, Y. Abe, M. Kawatsura, K. Suzuki, M. Mizuno, Y. Amano and T. Itoh, *Chemsuschem*, 2012, **5**, 388-391.
33. N. Sun, R. Parthasarathi, A. M. Socha, J. Shi, S. Zhang, V. Stavila, K. L. Sale, B. A. Simmons and S. Singh, *Green Chem.*, 2014, **16**, 2546-2557.
34. Q.-P. Liu, X.-D. Hou, N. Li and M.-H. Zong, *Green Chem.*, 2012, **14**, 304-307.
35. P. D. de Maria, *J. Chem. Technol. Biotechnol.*, 2014, **89**, 11-18.
36. S. Tang, G. A. Baker, S. Ravula, J. E. Jones and H. Zhao, *Green Chem.*, 2012, **14**, 2922-2932.

37. R. C. Remsing, R. P. Swatloski, R. D. Rogers and G. Moyna, *Chem. Commun. (Cambridge, U. K.)*, 2006, DOI: 10.1039/B600586C, 1271-1273.
38. T. G. A. Youngs, J. D. Holbrey, M. Deetlefs, M. Nieuwenhuyzen, M. F. Costa Gomes and C. Hardacre, *ChemPhysChem*, 2006, **7**, 2279-2281.
39. M. E. Zakrzewska, E. Bogel-Lukasik and R. Bogel-Lukasik, *Energy Fuels*, 2010, **24**, 737-745.
40. M. Isik, H. Sardon and D. Mecerreyes, *Int. J. Mol. Sci.*, 2014, **15**, 11922-11940.
41. K. M. Gupta and J. Jiang, *Chem. Eng. Sci.*, 2015, **121**, 180-189.
42. T. V. Doherty, M. Mora-Pale, S. E. Foley, R. J. Linhardt and J. S. Dordick, *Green Chem.*, 2010, **12**, 1967-1975.
43. D. Xu, Q. Yang, B. Su, Z. Bao, Q. Ren and H. Xing, *The Journal of Physical Chemistry B*, 2014, **118**, 1071-1079.
44. L. K. J. Hauru, M. Hummel, A. W. T. King, I. Kilpelainen and H. Sixta, *Biomacromolecules*, 2012, **13**, 2896-2905.
45. J. Shi, K. Balamurugan, R. Parthasarathi, N. Sathitsuksanoh, S. Zhang, V. Stavila, V. Subramanian, B. A. Simmons and S. Singh, *Green Chem.*, 2014, **16**, 3830-3840.
46. Y. Zhao, X. Liu, J. Wang and S. Zhang, *Carbohydr. Polym.*, 2013, **94**, 723-730.
47. B. Lu, A. Xu and J. Wang, *Green Chem.*, 2014, **16**, 1326-1335.
48. B. D. Rabideau, A. Agarwal and A. E. Ismail, *J. Phys. Chem. B*, 2014, **118**, 1621-1629.
49. H. Liu, K. L. Sale, B. M. Holmes, B. A. Simmons and S. Singh, *J. Phys. Chem. B*, 2010, **114**, 4293-4301.
50. B. Mostofian, J. C. Smith and X. Cheng, *Cellulose*, 2014, **21**, 983-997.
51. M. A. Tavanaie, *Chem. Eng. Technol.*, 2013, **36**, 1823-1837.
52. A. Figoli, T. Marino, S. Simone, E. Di Nicolo, X. M. Li, T. He, S. Tornaghi and E. Drioli, *Green Chem.*, 2014, **16**, 4034-4059.
53. A. Rezaei, A. Nasirpour and M. Fathi, *Compr. Rev. Food Sci. Food Saf.*, 2015, **14**, 269-284.
54. Y. Nishiyama, P. Langan and H. Chanzy, *J. Am. Chem. Soc.*, 2002, **124**, 9074-9082.
55. R. J. Moon, A. Martini, J. Nairn, J. Simonsen and J. Youngblood, *Chem. Soc. Rev.*, 2011, **40**, 3941-3994.
56. M. N. Belgacem and A. Gandini, in *Biopolymers – New Materials for Sustainable Films and Coatings*, John Wiley & Sons, Ltd, 2011, DOI: 10.1002/9781119994312.ch8, pp. 151-178.
57. S. Y. Ding and M. E. Himmel, *J. Agric. Food Chem.*, 2006, **54**, 597-606.
58. S.-Y. Ding, S. Zhao and Y. Zeng, *Cellulose*, 2014, **21**, 863-871.
59. D. J. Cosgrove, *Curr. Opin. Plant Biol.*, 2014, **22**, 122-131.
60. S.-Y. Ding, Y.-S. Liu, Y. Zeng, M. E. Himmel, J. O. Baker and E. A. Bayer, *Science*, 2012, **338**, 1055-1060.
61. R. H. Newman, *Solid State Nucl. Magn. Reson.*, 1999, **15**, 21-29.
62. M.-A. Ha, D. C. Apperley, B. W. Evans, I. M. Huxham, W. G. Jardine, R. J. Viëtor, D. Reis, B. Vian and Michael C. Jarvis, *The Plant Journal*, 1998, **16**, 183-190.
63. R. J. Viëtor, R. H. Newman, M.-A. Ha, D. C. Apperley and M. C. Jarvis, *The Plant Journal*, 2002, **30**, 721-731.
64. P. T. Larsson, K. Wickholm and T. Iversen, *Carbohydr. Res.*, 1997, **302**, 19-25.
65. Y. Pu, C. Ziemer and A. J. Ragauskas, *Carbohydr. Res.*, 2006, **341**, 591-597.
66. R. H. Atalla and D. L. VanderHart, *Solid State Nucl. Magn. Reson.*, 1999, **15**, 1-19.
67. C. Kennedy, G. Cameron, A. Šturcová, D. Apperley, C. Altaner, T. Wess and M. Jarvis, *Cellulose*, 2007, **14**, 235-246.
68. G. Sèbe, F. Ham-Pichavant, E. Ibarboure, A. L. C. Koffi and P. Tingaut, *Biomacromolecules*, 2012, **13**, 570-578.
69. T. Liitiä, S. Maunu, B. Hortling, T. Tamminen, O. Pekkala and A. Varhimo, *Cellulose*, 2003, **10**, 307-316.
70. R. H. Newman, *Holzforschung*, 1998, **52**, 157-159.

71. A. N. Fernandes, L. H. Thomas, C. M. Altaner, P. Callow, V. T. Forsyth, D. C. Apperley, C. J. Kennedy and M. C. Jarvis, *Proc. Natl. Acad. Sci. U. S. A.*, 2011, **108**, E1195-E1203.
72. K. Leppänen, S. Andersson, M. Torkkeli, M. Knaapila, N. Kotelnikova and R. Serimaa, *Cellulose*, 2009, **16**, 999-1015.
73. H. F. Jakob, D. Fengel, S. E. Tschegg and P. Fratzl, *Macromolecules*, 1995, **28**, 8782-8787.
74. S. Andersson, R. Serimaa, M. Torkkeli, T. Paakkari, P. Saranpää and E. Pesonen, *J. Wood Sci.*, 2000, **46**, 343-349.
75. R. H. Newman, S. J. Hill and P. J. Harris, *Plant Physiol.*, 2013, **163**, 1558-1567.
76. J. I. Langford and A. J. C. Wilson, *J. Appl. Crystallogr.*, 1978, **11**, 102-113.
77. P. Mansikkamäki, M. Lahtinen and K. Rissanen, *Carbohydr. Polym.*, 2007, **68**, 35-43.
78. L. H. Thomas, V. T. Forsyth, A. Šturcová, C. J. Kennedy, R. P. May, C. M. Altaner, D. C. Apperley, T. J. Wess and M. C. Jarvis, *Plant Physiol.*, 2013, **161**, 465-476.
79. T. G. A. Youngs, C. Hardacre and J. D. Holbrey, *J. Phys. Chem. B*, 2007, **111**, 13765-13774.
80. T. G. A. Youngs, J. D. Holbrey, C. L. Mullan, S. E. Norman, M. C. Lagunas, C. D'Agostino, M. D. Mantle, L. F. Gladden, D. T. Bowron and C. Hardacre, *Chem. Sci.*, 2011, **2**, 1594-1605.
81. A. S. Gross, A. T. Bell and J.-W. Chu, *J. Phys. Chem. B*, 2011, **115**, 13433-13440.
82. K. M. Gupta, Z. Hu and J. Jiang, *Polymer*, 2011, **52**, 5904-5911.
83. B. D. Rabideau, A. Agarwal and A. E. Ismail, *J. Phys. Chem. B*, 2013, **117**, 3469-3479.
84. G. Cheng, P. Varanasi, C. Li, H. Liu, Y. B. Menichenko, B. A. Simmons, M. S. Kent and S. Singh, *Biomacromolecules*, 2011, **12**, 933-941.
85. J. Zhang, X. Zhang, C. Li, W. Zhang, J. Zhang, R. Zhang, Q. Yuan, G. Liu and G. Cheng, *RSC Adv.*, 2015, **5**, 36999-37005.
86. B. Mostofian, J. C. Smith and X. Cheng, *Interdiscip. Sci.: Comput. Life Sci.*, 2011, **3**, 308-320.
87. A. S. Gross, A. T. Bell and J.-W. Chu, *Phys. Chem. Chem. Phys.*, 2012, **14**, 8425-8430.
88. J. M. Andanson, A. A. H. Padua and M. F. Costa Gomes, *Chem. Commun. (Cambridge, U. K.)*, 2015, **51**, 4485-4487.
89. H. F. N. de Oliveira and R. Rinaldi, *ChemSusChem*, 2015, **8**, 1577-1584.
90. L. Wu, S.-H. Lee and T. Endo, *Bioresour. Technol.*, 2013, **140**, 90-96.
91. P. Weerachanchai and J.-M. Lee, *ACS Sustainable Chem. Eng.*, 2013, **1**, 894-902.
92. F. Huo, Z. Liu and W. Wang, *J. Phys. Chem. B*, 2013, **117**, 11780-11792.
93. Y. Zhao, X. Liu, J. Wang and S. Zhang, *J. Phys. Chem. B*, 2013, **117**, 9042-9049.
94. J.-M. Andanson, E. Bordes, J. Devemy, F. Leroux, A. A. H. Padua and M. F. C. Gomes, *Green Chem.*, 2014, **16**, 2528-2538.
95. S. Velioglu, X. Yao, J. Devemy, M. G. Ahunbay, S. B. Tantekin-Ersolmaz, A. Dequidt, M. F. C. Gomes and A. A. H. Padua, *J. Phys. Chem. B*, 2014, **118**, 14860-14869.
96. S. Tang, G. A. Baker and H. Zhao, *Chem. Soc. Rev.*, 2012, **41**, 4030-4066.
97. H. Zhao, G. A. Baker, Z. Song, O. Olubajo, T. Crittle and D. Peters, *Green Chem.*, 2008, **10**, 696-705.
98. H. Zhao, C. L. Jones and J. V. Cowins, *Green Chem.*, 2009, **11**, 1128-1138.
99. Z. Chen, S. Liu, Z. Li, Q. Zhang and Y. Deng, *New J. Chem.*, 2011, **35**, 1596-1606.
100. A. Michud, M. Hummel, S. Haward and H. Sixta, *Carbohydr. Polym.*, 2015, **117**, 355-363.
101. S. Karatzos, L. Edye and R. Wellard, *Cellulose*, 2012, **19**, 307-312.
102. M. T. Clough, K. Geyer, P. A. Hunt, S. Son, U. Vagt and T. Welton, *Green Chem.*, 2015, **17**, 231-243.
103. J. R. Collier, J. L. Watson, B. J. Collier and S. Petrovan, *J. Appl. Polym. Sci.*, 2009, **111**, 1019-1027.
104. Q.-L. Kuang, J.-C. Zhao, Y.-H. Niu, J. Zhang and Z.-G. Wang, *J. Phys. Chem. B*, 2008, **112**, 10234-10240.
105. M. Gericke, K. Schlufter, T. Liebert, T. Heinze and T. Budtova, *Biomacromolecules*, 2009, **10**, 1188-1194.
106. X. Chen, Y. Zhang, L. Cheng and H. Wang, *J. Polym. Environ.*, 2009, **17**, 273-279.

107. H. Song, Y. Niu, Z. Wang and J. Zhang, *Biomacromolecules*, 2011, **12**, 1087-1096.
108. X. Chen, Y. Zhang, H. Wang, S.-W. Wang, S. Liang and R. H. Colby, *J. Rheol. (Melville, NY, U. S.)*, 2011, **55**, 485-494.
109. F. Lu, J. Song, B.-W. Cheng, X.-J. Ji and L.-J. Wang, *Cellulose*, 2013, **20**, 1343-1352.
110. R. Sescousse, K. A. Le, M. E. Ries and T. Budtova, *J. Phys. Chem. B*, 2010, **114**, 7222-7228.
111. S. J. Haward, V. Sharma, C. P. Butts, G. H. McKinley and S. S. Rahatekar, *Biomacromolecules*, 2012, **13**, 1688-1699.
112. F. Lu, B. Cheng, J. Song and Y. Liang, *J. Appl. Polym. Sci.*, 2012, **124**, 3419-3425.
113. S. Gebhard, *A Practical Approach to Rheology and Rheometry*, Gebrueder HAAKE GmbH, D-76227 Karlsruhe, Dieselstrasse 4, Germany, 2nd edn., 2000.
114. M. A. Rao, *Rheology of Fluid and Semisolid Foods: Principles and Applications*, Aspen Publishers, Gaithersburg, MD, 1990.
115. M. Rubinstein and R. H. Colby, *Polymer Physics,* , Oxford University Press 2003.
116. J. D. Ferry, *Viscoelastic Properties of Polymers*, Wiley, New York, 1980.
117. Q. Kuang, J. Zhang and Z. Wang, *J. Phys. Chem. B*, 2007, **111**, 9858-9863.
118. L. Wang, L. Gao, B. Cheng, X. Ji, J. Song and F. Lu, *Carbohydr. Polym.*, 2014, **110**, 292-297.
119. Y. Lv, J. Wu, J. Zhang, Y. Niu, C.-Y. Liu, J. He and J. Zhang, *Polymer*, 2012, **53**, 2524-2531.
120. A. Potthast, T. Rosenau, R. Buchner, T. Röder, G. Ebner, H. Bruglachner, H. Sixta and P. Kosma, *Cellulose*, 2002, **9**, 41-53.
121. Y. Chen, Y. Zhang, F. Ke, J. Zhou, H. Wang and D. Liang, *Polymer*, 2011, **52**, 481-488.
122. S. V. Troshenkova, E. S. Sashina, N. P. Novoselov and K. F. Arndt, *Russ. J. Gen. Chem.*, 2010, **80**, 501-506.
123. F. Nemoto, M. Kofu and O. Yamamuro, *J. Phys. Chem. B*, 2015, **119**, 5028-5034.
124. T. Singh and A. Kumar, *J. Phys. Chem. B*, 2007, **111**, 7843-7851.
125. H. C. Zhang, K. Li, H. J. Liang and J. J. Wang, *Colloids Surf., A*, 2008, **329**, 75-81.
126. D. M. Rein, R. Khalfin, N. Szekely and Y. Cohen, *Carbohydr. Polym.*, 2014, **112**, 125-133.
127. T. Chatterjee, A. I. Nakatani, R. Adden, M. Brackhagen, D. Redwine, H. Shen, Y. Li, T. Wilson and R. L. Sammler, *Biomacromolecules*, 2012, **13**, 3355-3369.
128. J. R. Lott, J. W. McAllister, M. Wasbrough, R. L. Sammler, F. S. Bates and T. P. Lodge, *Macromolecules*, 2013, **46**, 9760-9771.
129. J. R. Lott, J. W. McAllister, S. A. Arvidson, F. S. Bates and T. P. Lodge, *Biomacromolecules*, 2013, **14**, 2484-2488.
130. K. Kuroda, H. Kunimura, Y. Fukaya and H. Ohno, *Cellulose*, 2014, **21**, 2199-2206.
131. H. Cruz, M. Fanselow, J. D. Holbrey and K. R. Seddon, *Chem. Commun. (Cambridge, U. K.)*, 2012, **48**, 5620-5622.